Energy Conversion and Management 84 (2014) 41–49

Contents lists available at ScienceDirect

Energy Conversion and Management

journal homepage: www.elsevier.com/locate/enconman

Experimental study and performance analysis of a thermoelectric cooling and heating system driven by a photovoltaic/thermal system in summer and winter operation modes

Wei He [a,*], JinZhi Zhou [a], Chi Chen [b], Jie Ji [a]

[a] Department of Thermal Science and Energy Engineering, University of Science and Technology of China, Jinzhai Road 96, Hefei 230026, China
[b] Department of Mechanical Engineering, The Hong Kong University of Science and Technology, Hong Kong Special Administrative Region

ARTICLE INFO

Article history:
Received 31 December 2013
Accepted 4 April 2014
Available online 4 May 2014

Keywords:
Heat pipe PV/T system
Thermoelectric
COP
Electrical efficiency
Thermal efficiency
Energetic efficiency
Exergetic efficiency

ABSTRACT

This paper presents theoretical and experimental investigations of the winter operation mode of a thermoelectric cooling and heating system driven by a heat pipe photovoltaic/thermal (PV/T) panel. And the energy and exergy analysis of this system in summer and winter operation modes are also done. The winter operation mode of this system is tested in an experimental room which temperature is controlled at 18 °C. The results indicate the average coefficient of performance (COP) of thermoelectric module of this system can be about 1.7, the electrical efficiency of the PV/T panel can reach 16.7%, and the thermal efficiency of this system can reach 23.5%. The energy and exergy analysis show the energetic efficiency of the system in summer operation mode is higher than that of it in winter operation mode, but the exergetic efficiency in summer operation mode is lower than that in winter operation mode, on the contrary.

1. Introduction

In the past decades, because of the development of the economic and industrial, the non-renewable and polluting fossil fuels were consumed largely. And it is necessary to explore new energy to remit the needing pressure of energy. The solar energy is a new way to relieve the pressure, because it is pollution free and easy to gain. Many devices have been designed to gain solar energy. Flat-plate solar collector is steady and efficient and it has been widely used in residential water, space heating and commercial or industrial applications. Its efficiency can be improved by reducing its size and obtaining higher temperature fluid at outlet. There are many different highly-effective techniques which have been used in the past to enhance the thermal performance of solar collectors including the methods of reducing the heat loss from the top surface [1,2] or increasing the energy gain inside the solar converter [3,4]. The building-integrated dual-function solar collector is a new structure collector which can perform in two different modes: working as a passive space heating collector in cold sunny days such as in winter or working as a facade water heating collector in hot days such as in summer [5–7].

The PV/T system has been researched widely because it can use solar energy more sufficiently to produce electrical and thermal energy simultaneously. Henning Helmers and Korbinian Kramer presented a performance model that enables yield predictions of hybrid photovoltaic and thermal (PVT) collectors. It applied for both non-concentrating (PVT) and concentrating (CPVT) systems. The model was based on considerations of energy balance, heat transfer and the dependence of the photovoltaic efficiency on absorber temperature and applied to measurement data of a CPVT collector to exemplify the procedure and to validate the model [8]. Faizal reported the energy, economic and environmental analysis of metal oxides nanofluid for flat-plate solar collector which used nanofluid as working fluid. From the study, it was estimated that a large number of solar collectors can be saved for CuO, SiO_2, TiO_2 and Al_2O_3 nanofluid. The average value of 220 MJ embodied energy can be saved for each collector, 2.4 years payback period can be achieved and around 170 kg less CO_2 emissions in average can be offset for the nanofluid based solar collector compared to a conventional solar collector [9]. da Silva and Fernandes researched the thermodynamic modeling of hybrid photovoltaic–thermal (PV/T) solar systems, pursuing a modular strategy approach provided by Simulink/Matlab. And the results showed that the modular approach strategy provided by Matlab/Simulink was applicable to solar systems modeling, providing better code scalability, faster developing time, and simpler integration with

* Corresponding author.
E-mail address: hwei@ustc.edu.cn (W. He).

http://dx.doi.org/10.1016/j.enconman.2014.04.019
0196-8904/

Nomenclature

A	contact area, m^2
C_p	heat capacit, J/(kg K)
$\dot{E}_{pv}$	photovoltaic output power per unit cell area, W/m^2
$\dot{E}_{te}$	thermal output power per unit collector area, W/m^2
$\dot{E}\chi_{pv}$	photovoltaic exergy output per unit PV cell area, W/m^2
$\dot{E}\chi_{te}$	thermal exergy output per unit collector area, W/m^2
$\dot{E}\chi_{sun}$	exergy input of solar radiation, W/m^2
G_T	solar irradiance, W/m^2
I	current, A
K	thermal conductivity, W/(kg K)
L	thickness, m
M	quality, kg
P	power, W
Q	Heat flux, W
R	thermal resistance, K/W
R'	thermal contact resistance, K/W
R''	contact resistance coefficient, m^2 K/W
S	area, m^2
T	temperature, K
ΔT	temperature variation of water, °C
U	voltage, V
α	absorptivity or Seebeck coefficient thermoelectric materials, V/K
β	Boltzmann's constant, W/(m^2 K^4)
ε	Exergetic efficiency
η_{te}	thermal efficiency of the system
η_{pv}	electrical efficiency of solar cells
η_{pvt}	total efficiency of the system
κ_{panel}	emissivity of absorber panel
σ	conductivity of the thermoelectric materials, s/m
τ	Interval time of data collection, s
ξ	PV cell packing, factor

Subscripts

1	ceramic shell of thermoelectric device
2	radiator
3	foam wall
4	brick wall
5	copper plate
6	water block
a	ambient environment
c	cold side of thermoelectric module
h	hot side of thermoelectric module
heat-hr	hot side of thermoelectric module and experimental room
heat-cw	cold side of thermoelectric module and heating water
n	number
pipe-t	top of heat pipe
pipe-m	middle of heat pipe
pipe-b	bottom of heat pipe
panel	absorber panel
r	experimental room
s	thermoelectric module
solar	PV cell
t	thermoelement
te	thermal energy
w	water in the storage tank

external computational tools, when compared with traditional imperative-oriented programming languages [10]. Highly thermal efficiency can be achieved via the combination of solar collector and other devices. The composite structure of solar collector and heat pump is common one. José Fernández-Seara and Carolina Piñeiro reported the experimental analysis of a direct expansion solar assisted heat pump with integral storage tank for domestic water heating under zero solar radiation conditions [11]. Moreno-Rodríguez and González-Gil presented the theoretical model and experimental validation of a direct-expansion solar assisted heat pump for domestic hot water (DHW) applications. The acquired experimental coefficient of performance was found to be in the rank of 1.7–2.9.The DHW tank temperature over the course of the study is 51 °C[12]. S.K. Chaturvedi researched the solar-assisted heat pump which was sustainable for low-temperature water heating applications. Results indicated that the DX-SAHP (Direct expansion solar assisted heat pump) water heaters systems when compared to the conventional electrical water heaters were both economical as well as energy conserving. The analysis also revealed that the minimum value of the system life cycle cost was achieved at optimal values of the solar collector area as well as the compressor displacement capacity [13]. Gang and Huide presented a dynamic model of a heat pipe PV/T system and constructed a test rig. Experiments were conducted to validate the results of the simulation. Based on the validated module, the performances of the heat pipe PV/T system were studied under different parametric conditions, such as water flow rates, PV cell covering factor of the collector, tube space of heat pipes, and kinds of solar absorptive coatings of the absorber plate [14].

Solar thermoelectric refrigerator were reported by many researchers [15–17], but thermoelectric heating was not a common research field. This article introduced the application of combining of PV/T system, thermoelectric modules and building. The summer operation mode of the system which can provide cooling for room and heat domestic hot water for user was tested with the small-scale version [18]. The results indicate the system has a higher electrical efficiency (15.4%) and thermal efficiency (29.4%), and the thermoelectric module has a strong cooling ability that COP is about 0.45. Now the experimental performance and theoretical analysis of the system in winter operation mode are presented in this paper. And energy and exergy analysis are also done in summer and winter operation modes, which are validated by the small-scale system and this paper.

2. Experimental structure and working principles of the system

2.1. Experimental structure

The experimental structure of the thermoelectric heating system driven by a heat pipe PV/T panel is shown in Figs. 1 and 2.

The system is composed of a heat pipe PV/T panel, model of maximum power point tracking and controling the solar charge, experimental room, thermoelectric modules, heat exchangers, pumps, fans and storage tank. The experiment was carried out on the sunny days of winter. The dates which were recorded include the temperature of the PV/T panel, heat pipe, the cold side and hot side of thermoelectric modules, the experimental room and comparative room, ambient and the water of storage tank, the solar irradiance, the output Voltage and current of the PV/T system, the input Voltages and currents of thermoelectric modules, the amount electricity used in the experimental and comparative room in which EHS used. The difference of the mathematical models between the summer operation mode and winter operation mode is that the direction of current input is opposite, hence the hot side

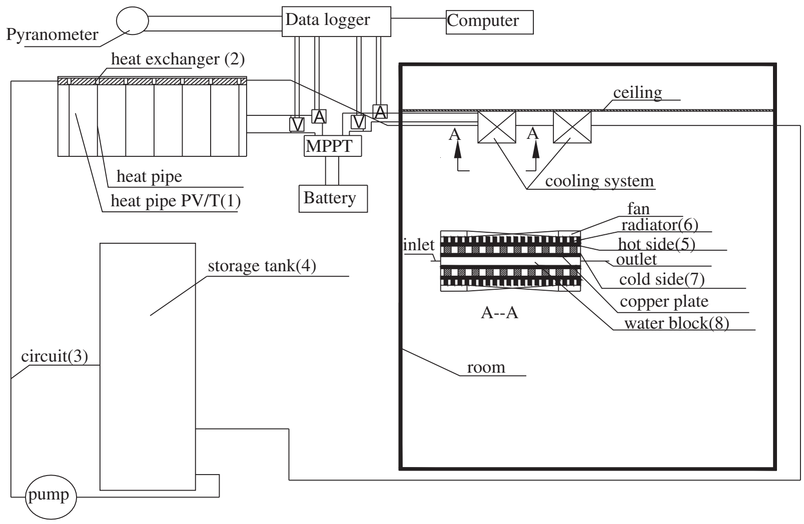

Fig. 1. Experimental structure of system.

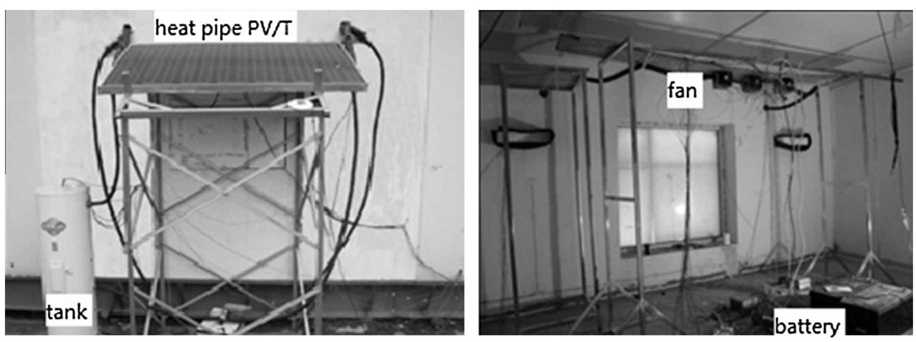

Fig. 2. Experimental installations.

in summer which release heat to cooling water is the cold side in winter which absorbs heat from the heating water, and the cold side in summer which absorbs heat from the experimental room is the hot side in winter which release heat to room. The difference of the system in winter operation mode is that there are four thermoelectric modules (six modules in summer) and 30 L (150 L in summer) water is used in the experiment, and the temperature of experimental in winter is set at 18 °C (26 °C in summer).

2.1.1. Heat pipe PV/T panel

The effective irradiation-collection area of the HP-PV/T solar collector is 1.95 m^2, and the PV cell area is 1.53 m^2. The structure of it is showed in Fig. 3. The PV modules comprise 98 pieces of small PV cells that are arranged in series with dimensions of125 × 125 mm, and its photovoltaic characteristics under standard test conditions (at irradiationintensity of 1000 W/m^2 and temperature of 25 °C)are presented in Table 1.

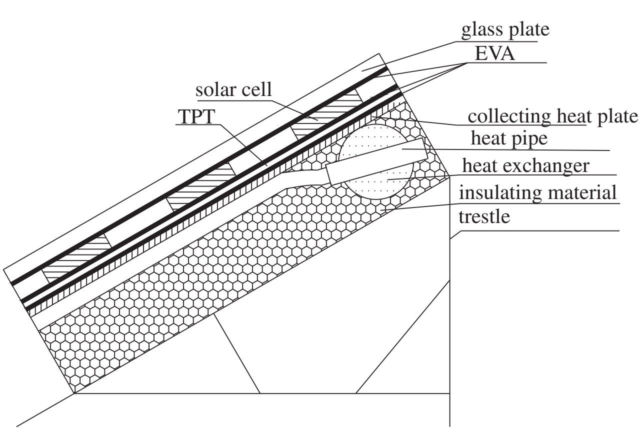

Fig. 3. Construction of the heat pipe PV/T.

Table 1
The performance parameters of it.

Heat pipe PV/T panel	$\eta_{T_{ref}}$	P_{max} (W)	U_{mp} (V)	I_{mp} (A)	U_{oc} (V)	I_{sc} (A)
	18%	272	49.5	5.49	59.4	5.94

2.1.2. Model of maximum power point tracking solar charge controller

The model of maximum power point tracking solar charge controller (MPPT) is Tracer-2210RN. The performance parameters of it are showed in Table 2.

The tracer series controller is for off-grid solar systems and it controls the charging and discharging of the battery. It is especially suitable for the thermoelectric modules systems. The controller features a smart tracking algorithm inside that maximizes the energy from the solar PV module and charges the battery. The low voltage disconnect function prevents the battery from over discharging.

2.1.3. Indoor temperature control system within the experimental and comparative rooms

The indoor temperature controller system in the experimental room and comparative room consist of two parts: an

Table 2
Performance parameters of MPPT.

MPPT	System voltage	Rated battery current rate	Load current	Max. PV input voltage	Max. PV input Power
	12/24VDC20A20A	100VDC	260 W		

air-conditioner system that supplies cooling capacity and records the amount of heat removed from the indoor area and an electrical heating system (EHS) that supplies heating capacity and records the amount of heat released into the indoor area. These two systems work together to maintain the temperature at desired setting. The heating ability of the thermoelectric modules can be calculated by the difference between the heats removed and released.

2.2. Working principle of the system in winter

The working principle of the system in winter is showed in Fig. 1. The heat pipe PV/T panel (1) is located outside of the experimental room. It is combined with the heat exchanger (2) via heat pipes. Inside of the experimental room, the hot sides of the thermoelectric modules (5) are connected to the radiators (6), and the cold sides of the modules (7)are connected with the water blocks (8).The water blocks (8), storage tank (4) and heat exchanger (2)are connected together via circuit (3). When the system works, the water flows through heat exchanger (2), water blocks (8) and then back to storage tank (4). The heat pipe PV/T panel (1) heats the circulating water in the heat exchanger (2) via heat pipes, and then the cold sides of thermoelectric modules (5) absorb heat from the circulating water. The hot sides of thermoelectric modules (5) release heat to the experimental room via radiators (6) and fans.

3. Mathematical models and error analysis

3.1. The heat balance between the hot side of thermoelectric module and experimental room is expressed as follows

$$Q_{heat\text{-}hr} = \frac{T_h - T_r}{R_1 + R'_{12} + R_2} \tag{1}$$

Here, $Q_{heat\text{-}hr}$ is the heat transfer between the hot side of the thermoelectric module and the experimental room, and T_h is the temperature of the hot side of thermoelectric module, T_r is the temperature of the experimental room. R_1 is the thermal resistance of the ceramic shell of thermoelectric module. R'_{12} is the thermal contact resistance between the thermoelectric module and radiator, R_2 is the thermal resistance of the radiator.

3.2. The construct of the cooling system is showed in Fig. 4

The heat balance between the cold side of thermoelectric module and heating water is expressed as follows:

$$Q_{heat-cw} = \frac{T_w - T_c}{R_1 + R_5 + R_6 + R'_{15} + R'_{56}} \tag{2}$$

Here, $Q_{heat-cw}$ is the heat transfer between the cold side of thermoelectric module and heating water. T_w is the temperature of heating water. T_c is the temperature of the cold side of thermoelectric module, R_5 is the thermal resistance of copper plate. R_6 is the thermal resistance of wall of water block. R'_{15} is the thermal contact resistance between the ceramic and copper plate. R'_{56} is the thermal contact resistance between the copper plate and water block (see Fig. 4).

3.3. Coefficient of performance (COP) of the thermoelectric module

$$\mathrm{COP} = \frac{Q_h}{U_t I_t} \tag{3}$$

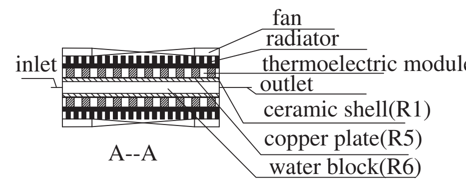

Fig. 4. Construct of the cooling system.

Here, Q_h is the heat released by the hot side of thermoelectric module. $U_t I_t$ is the input power of the thermoelectric module.

3.4. Electrical efficiency of the heat pipe PV/T [19]

$$\eta_{pv} = \eta_{T_{ref}}[1 - 0.0045(T_{solar} - 298.15)] \tag{4}$$

Here, η_{pv} is the electrical efficiency. $\eta_{T_{ref}}$ is the module's electrical efficiency at the reference temperature which is 0.18. T_{solar} is the module operating temperature.

3.5. The thermal efficiency of the system

$$\eta_{te} = \frac{Q_{\tan k} + \sum_{n=1}^{n=n_{solar}} n_s Q_{hi}}{\sum_{n=1}^{n=n_{solar}} G_{Ti} \tau S_{panel}} \tag{5}$$

Here, η_{te} is the thermal efficiency of the system. Q_{tank} is the heat that the water in storage tank has gained. $\sum_{n=1}^{n=n_{solar}} n_s Q_{hi}$ is the heat which the thermoelectric modules released. $Q_{\tan k} + \sum_{n=1}^{n=n_{solar}} n_s Q_{hi}$ is the total heat which the system has released. G_{Ti} is the solar radiation flux (irradiance) on module plane. τ is the time interval of data collection. S_{panel} is the area of the absorber plate. n_{solar} is the number of the data has been recorded. $\sum_{n=1}^{n=n_{solar}} G_{Ti} \tau S_{panel}$ is the total energy which the PV/T panel has gained.

3.6. The energy and exergy analysis of the heat pipe PV/T system

From the first law of thermodynamics, the energetic efficiency of the system η_{pvt} is composed by two parts: the electrical efficiency η_{pv} and thermal efficiency η_{te}, and the equation are given as follows [20]:

$$\eta_{pvt} == \frac{\int_{t_1}^{t_2} (S_{panel} \dot{E}_{te} + S_{solar} \dot{E}_{pv}) dt}{S_{panel} \int_{t_1}^{t_2} G_T dt} = \xi \eta_{pv} + \eta_{te} \tag{6}$$

$$\xi = \frac{S_{solar}}{S_{panel}} \tag{7}$$

Here, $\dot{E}_{pv}$ is the photovoltaic output power per unit cell area. $\dot{E}_{te}$ is the thermal output power per unit collector area. G_T is the solar irradiation per unit collector area. ξ is the PV cell packing factor.

The first law of thermodynamics assessed the performance of the PV/T system, however, these assessments cannot perfectly describe the performance of it, because only under the condition of existing a temperature difference between a high-temperature heat source and a low-temperature heat sink, can the thermal energy produce work. Thus, the exergy analysis was based on the second law of thermodynamics, which revealed a system with a reasonable degree of energy and can better evaluate the perfor-

mance of the PV/T system. The exergetic efficiency can be defined as follows [21]:

$$\varepsilon_{pvt} = \frac{\int_{t_1}^{t_2} (S_{panel}\dot{E}\chi_{te} + S_{solar}\dot{E}\varphi_{pv})dt}{S_{panel}\int_{t_1}^{t_2} \dot{E}\chi_{sun}dt} = \xi\varepsilon_{pv} + \varepsilon_{te} \tag{8}$$

$$\dot{E}\chi_{pv} = \dot{E}_{pv} \tag{9}$$

$$\dot{E}\chi_{te} = \dot{E}_{te}\left(1 - \frac{T_a}{T_{\tan k}}\right) \tag{10}$$

$$\dot{E}\chi_{sun} = \left[1 + \frac{1}{3}\left(\frac{T_a}{T_{sun}}\right)^4 - \frac{4T_a}{3T_{sun}}\right]G_T \tag{11}$$

Here, $\dot{E}\chi_{pv}$ is the photovoltaic exergy output per unit PV cell area. $\dot{E}\chi_{te}$ is the thermal exergy output per unit collector area. $\dot{E}\chi_{sun}$ is the exergy input of solar radiation. T_{sun} is the solar radiation temperature which is 6000 K.

3.7. The energy transfer process of the system

The current of the thermoelectric module [22]:

$$\Omega_t = n_t\left(\frac{l_n}{\sigma_n S_n} + \frac{l_p}{\sigma_p S_p}\right) \approx \frac{2n_t l_t}{\sigma_n S_n} \tag{12}$$

$$I_t = \frac{U_t}{R_t} = \frac{U_t \sigma_n S_n}{2n_t L_t} \tag{13}$$

Here, Ω_t is the resistance of the thermoelectric module. α is the Seebeck coefficient of thermoelectric materials (the p-type and the n-type assumed to be same), I_t is the current, S_t is the cross-sectional area, l_t is length of thermoelement, σ is the conductivity of the thermoelectric materials, n_t is the number of thermoelements U_t is the voltage of thermoelectric module.

The temperature of hot side of thermoelectric module:

$$Q_{h1} = \frac{T_{h2} - T_r}{R_{hot}} \Rightarrow T_{h2} = T_r + Q_{h1}R_{hot} \tag{14}$$

Here, R_{hot} is the total thermal resistance between the hot side of thermoelectric module and experimental room.

The temperature of cold side of thermoelectric module:

$$Q_{c1} = \frac{T_{w1} - T_{c2}}{R_{cold}} \Rightarrow T_{c2} = T_{w1} - Q_{c1}R_{cold} \tag{15}$$

Here, R_{cold} is the total thermal resistance between the cold side of thermoelectric module and water block.

The temperature of water in storage tank:

$$T_{w2} = T_{w1} + \Delta T = T_{w1} + \frac{\tau\left(U_{pump}I_{pump}\eta_{pump} + n_{pipe}\frac{T_{panel}-T_{w1}}{R_{pw}} - n_s Q_c - Q_{loss}\right)}{C_{pw}M_w} \tag{16}$$

Here, τ is the interval time of data collection. $U_{pump}I_{pump}\eta_{pump}$ is the heat which the pump released. R_{pw} is the total thermal resistance between the heat pipe PV/T panel and water in the heat exchanger. $n_{pipe}\frac{T_{panel}-T_{w1}}{R_{pw}}$ is the heat which was transferred from PV/T panel to the water in storage tank. $n_s Q_c$ is the heat which the thermoelectric modules absorbed. Q_{loss} is the total heat loss of storage tank and circulation line. $\tau(U_{pump}I_{pump}\eta_{pump} + n_{pipe}\frac{T_{panel}-T_{w1}}{R_{pw}} - n_s Q_c - Q_{loss})$ is the heat which storage tank gained in the interval time of data collection. A flow chart of this system is showed in Fig. 5.

According to the first section in Fig. 6, with the voltage ($U_{\rm pvt}$) and current ($I_{\rm pvt}$) which the heat pipe PV/T panel produces, actual power (P_{exp}) of PV/T system can be calculated, and then it will be compared with the theoretical power (P_{sim}) which can be calculated with Eq. (4). If the difference is within the setting range, it will continue to the second section, else it will return to the beginning.

During the second section, the current (I_{t1}) of the thermoelectric modules can be calculated with the voltage (U_{t1}) (Eqs. (12) and (13)) which the battery output. With the $T_{c1_{\exp}}$ and $T_{h1_{\exp}}$, the heat absorbed by cold side $Q_{c1_{sim}}$ and heat released by hot side $Q_{h1_{sim}}$ of thermoelectric module can be calculated. With the temperature of experimental room T_r and $Q_{h1_{sim}}$, the $T_{h2_{sim}}$ can be calculated (equation 14). With the temperature of water $T_{w1_{\exp}}$, and the $Q_{c1_{sim}}$, $Q_{heat-pw1_{\exp}}$, $T_{c2_{sim}}$ and $T_{w2_{sim}}$ be calculated (Eqs. (15) and (16)), then $T_{c2_{sim}}$, $T_{h2_{sim}}$ and $T_{w2_{sim}}$ will be compared with the experimental values. If the difference is within the setting range, the program will be finished, else it will return to the beginning.

3.8. Error analysis

The experimental error of the independent variables, such as temperature, output electricity and solar irradiation, is determined by the accuracy of the corresponding instrument. While the experimental error of the dependent variables, including the overall system heat gain, η_{pvt}, η_{pv} and η_{te} can be calculated from the experimental error of the independent variables according to the theory of error propagation.

The relative error (RE) of the dependent variable y is calculated as follows [21]:

$$\text{RE} = \frac{\text{d}y}{y} = \frac{\partial f}{\partial x_1}\frac{\partial x_1}{y} + \frac{\partial f}{\partial x_2}\frac{\partial x_2}{y} + \ldots \frac{\partial f}{x_n}\frac{\partial x_n}{y} \tag{17}$$

$$y = \int (x_1, x_2, \ldots x_n) \tag{18}$$

where x_i, ($i = 1 \ldots n$) is the variable of the dependent variable y, and $\partial f/\partial x$ is the error transferring coefficient of the variables.

The experimental relative mean error (RME) during the test period can be expressed as:

$$\text{RME} = \frac{\sum_1^N |Re|}{N} \tag{19}$$

Based on the Eqs. (21)–(23), The RME of all variables discussed is listed in Table 3.

4. Results and analysis

In the morning, with the solar irradiance increasing from 200 w/m^2 to 700 w/m^2, the output power of the heat pipe PV/T panel increased fast from 50 w to 170 w (shown in Fig. 6), and the temperature of the PV/T panel increases steady, hence the heat which the water has absorbed and the temperature of it both increase. The temperature of cold side of the thermoelectric module as a similar trend with the water, because it absorbs heat from the water, but the temperature of hot side of the thermoelectric module does not change obviously, since the heat which the cold side absorbs (As shown in Fig. 8, the difference of temperature between the water and the cold side is very steady, hence the heat transferred between them do not change nearly) and the input power of the thermoelectric module which has a steady input voltage supplied by battery (shown in Fig. 9) are both steady, and relationship between the heat release and the temperature of the hot side is nearly linear correlation (the current is steady).In the afternoon, with the solar irradiance decreasing from 700 w/m^2 to 300 w/m^2, the output power and the temperature of PV/T panel both decrease, but the temperature of panel (average 35 °C)is always higher than the water (average 21 °C), hence the temperature of water and cold side of thermoelectric module keep increas-

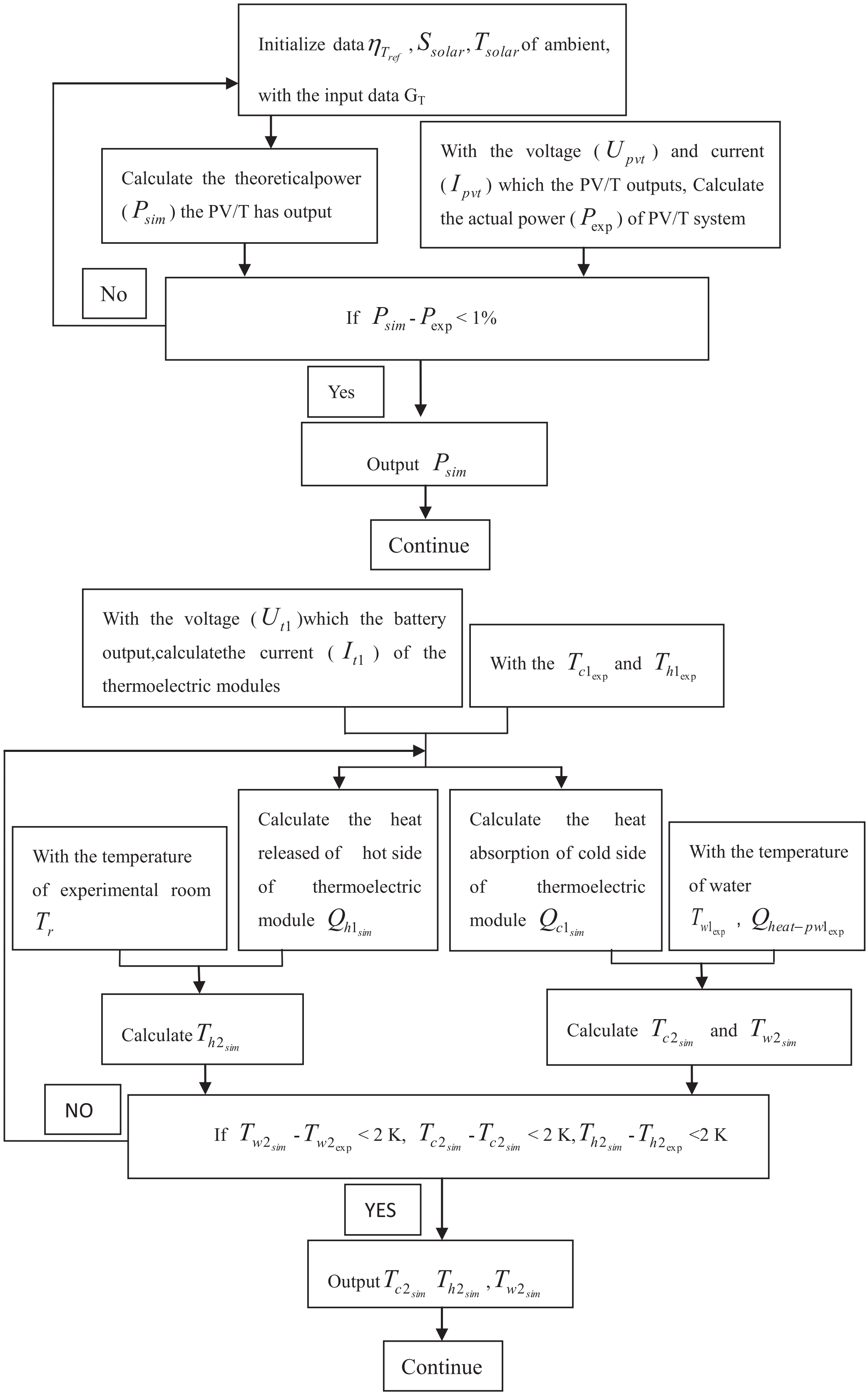

Fig. 5. Flow chart of simulation.

ing slowly, and the temperature of hot side keeps steady. The COP is stable before 11:00, and the reason is that the increasing rate of Q_h is similar with input power of thermoelectric module. With the temperature of water increasing, T_c and Q_c also increase, and the rate of increase is much faster. Q_h contains two parts: the Q_c and U_tI_t. The U_tI_t is very steady from 11:00 to 13:00, and then begins

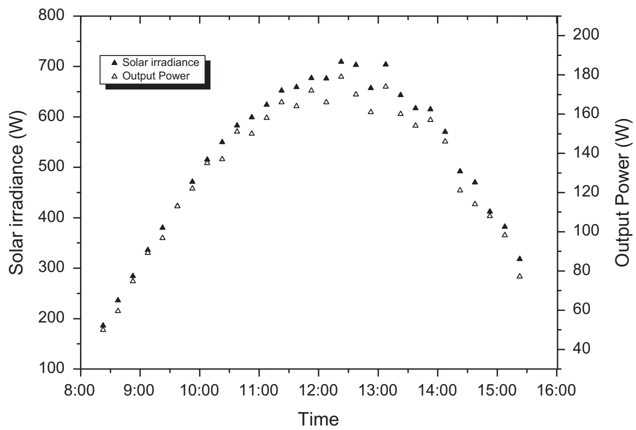

Fig. 6. Variations of output power and solar irradiance on a sunny day.

Table 3
Experimental RME of the variables.

Variable	T	G_T	η_{te}	η_{pv}	η_{pvt}
RME	0.0693%	1%	0.4%	0.09%	1.49%

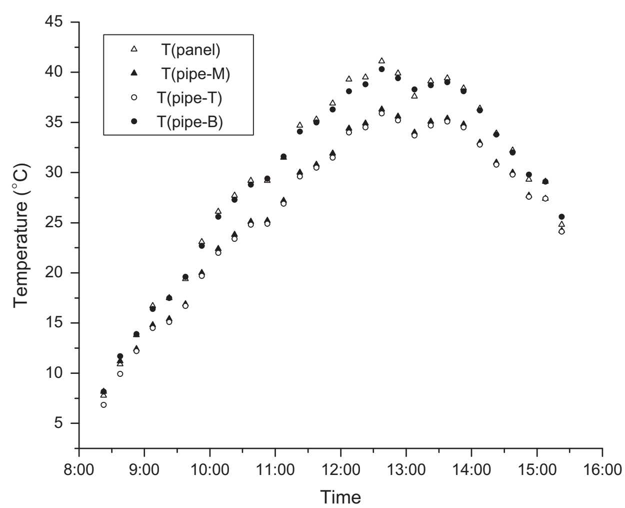

Fig. 7. Variations of the temperature of PV/T panel and heat pipe on a sunny day.

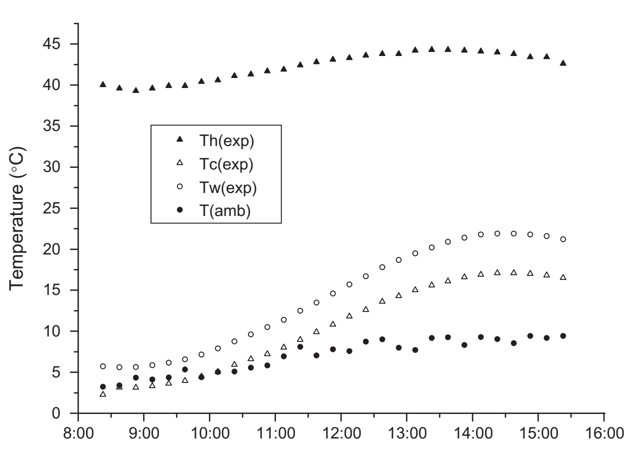

Fig. 8. Variations in T_h, T_c, T_w and ambient temperature T_{amb} on a sunny day.

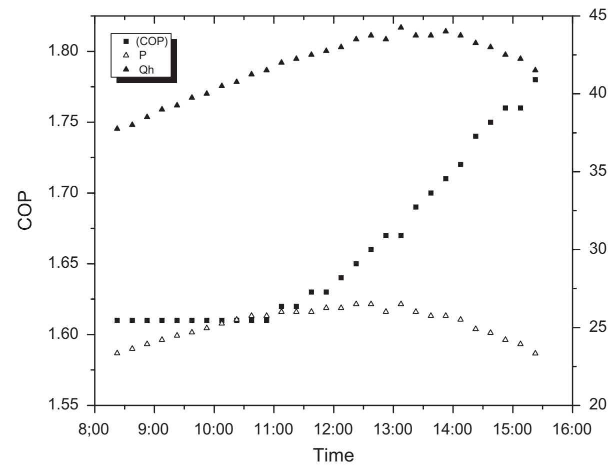

Fig. 9. Variations in the input power, COP and Q_h of the thermoelectric module.

to decrease. Q_C increases steadily from 11:00 to 16:00. Hence the COP ($COP = \frac{Q_h}{U_t I_t} = \frac{U_t I_t + Q_c}{U_t I_t}$) begins to increase from 11:00.

Fig. 7 shows the variation in temperature of heat pipe PV/T panel and heat pipe through all day. The temperature of the heat pipes in the bottom is highest, because it is the evaporator which absorbs heat from the panel. The temperature of the heat pipe at the top is lowest, because it is the condenser which releases heat into the water. The temperature in the middle is between that in the bottom and at the top, because the vapor turns into water when its heat is absorbed by the circulating water, and then the water returns back to the bottom of heat pipe with the force of gravity which will decrease the temperature of middle during the process.

As shown in The Fig. 10, the heat released by electrical heating system in experimental room and comparative room can be calculated. And all the data is shown in Table 4.

The simulated and experimental electrical efficiency of the heat pipe PV/T panel are showed in Fig. 11. The electrical efficiency is related to the temperature of the panel. The temperature of panel increases in the morning, peaking at noon. It decreases during the afternoon (Fig. 6). Electrical efficiency decreases in the morning, reaches its minimum at noon, and then begins to rise in the afternoon. The simulated and experimental electrical efficiency are founded to be correlated with each other, and the average values are17.6% and 16.7%.

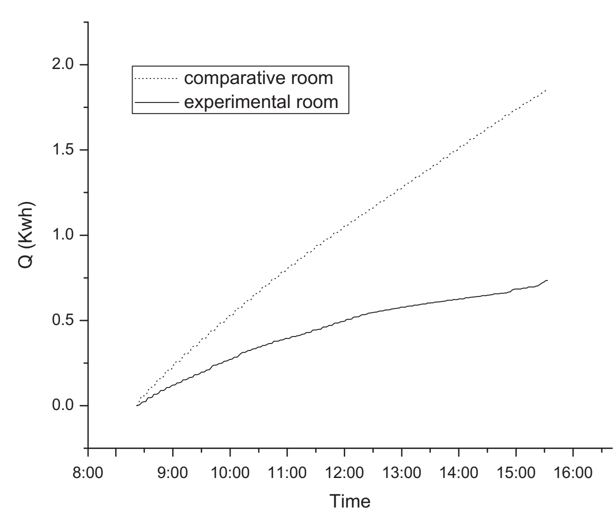

Fig. 10. Variation in the amount electricity used in the experimental and comparative room in which EHS used.

Table 4
Heat release comparison.

Room	Heat release of thermoelectric modules	Heat released of EHS	Heat transferred from ambient
Experiment	1.20(KW h)	0.735(KW h)	−1.935(KW h)
Comparative		1.855 (KW h)	−1.855(KW h)

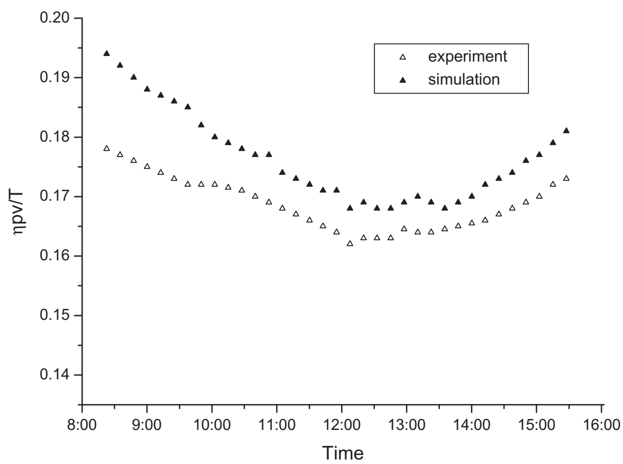

Fig. 11. Electrical efficiency of the heat pipe PV/T panel.

As shown in Figs. 12 and 13, all the simulative and experimental temperature of cold side, hot side of thermoelectric module and water in storage tank are corrected with each other, and the maximum deviation is lower than 1 °C. The temperature of water in storage tank increases by15.2 °C, and the simulated and experimental thermal efficiencyare23.9%and 23.5%, respectively.

The thermal efficiency of the system in winter operation mode is lower than it in summer operation mode. The main reason includes two factors: (1) there are six thermoelectric modules (total input power 156 W) used in summer which are powered by the heat pipe PV/T system (average output power 161 W). There are four thermoelectric modules (total input power 104 W) used in winter, and the average output power of the heat pipe PV/T system is 125 W. There is some electricity which is not used and stored in

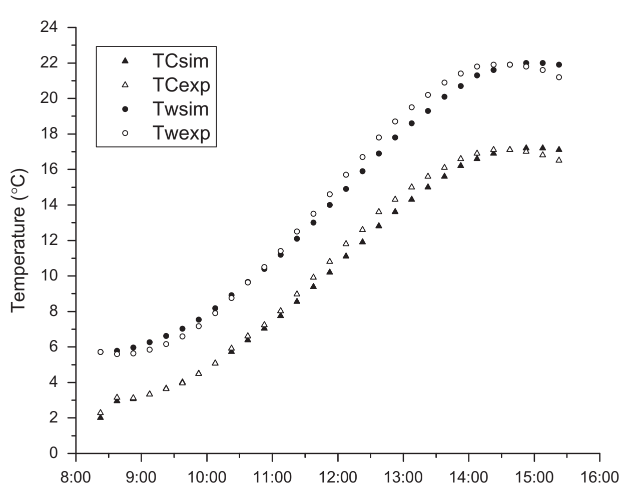

Fig. 12. Temperature of the cold side of thermoelectric module and the water in the storage tank.

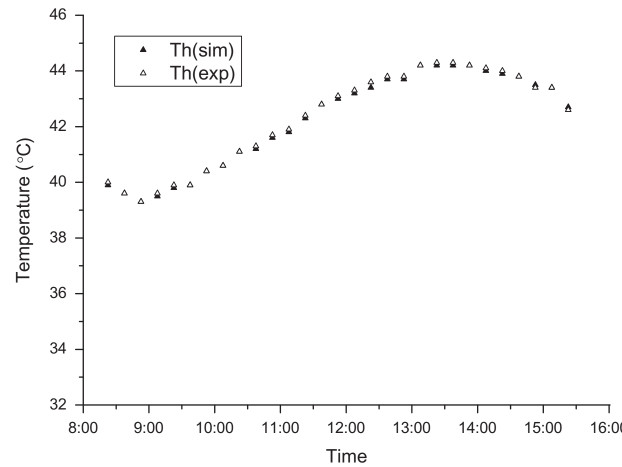

Fig. 13. Temperature of the hot side of thermoelectric module.

the battery, hence the heat thermoelectric modules releases decreased; (2) the thermal contact resistance is related to the temperature, and while the temperature is increasing, the thermal contact resistance is decreasing [23]. The temperature of the circulating water in winter operation mode(average 14 °C) is much lower than that in summer operation mode(average 31 °C), hence the ability of heat transfer between the heat pipe PV/T panel and the circulating water in winter operation mode is worse than that in summer operation mode.

The energetic efficiency of the heat pipe PV/T system in summer operation mode (41.49%) is higher than that in winter operation mode (36.6%), but the exergetic efficiency of the heat pipe PV/T system in summer operation mode (12.9%) is lower than that in winter operation mode (14.14%).The main influencing factor is the ambition temperature. The ambition temperature in winter (9 °C) is lower 20°Cthan that in summer (29 °C), hence the temperature of the panel in winter is lower than that in summer, and electrical efficiency of heat pipe PV/T system in winter (16.7%) is higher 1.3% than that in summer (15.4%). The thermal exergetic efficiency in winter (1.08%) is higher 0.27 than that in summer (0.81%).

5. The energy analysis of the heat pipe PV/T system in summer and winter

The energy analysis presented in this section is mainly based on the first law of thermodynamics. And the theoretical model based on thermal energy balance is employed for the study of the heat pipe PV/T system:

$$Q_{absorbed} = Q_{accumulated} + P_{used} + Q_{lost} \tag{20}$$

The absorbed energy:

$$Q_{absorbed} = G_T S_{panel} \tag{21}$$

The accumulated energy:

$$Q_{accumulated} = C_{p,c} M_{panel} \frac{dT_{panel}}{dt} \tag{22}$$

Here, $C_{p,c}$ and M_{panel} are the specific heat capacity and quality of absorber panel, respectively.

The useful energy:

$$P_{used} = \eta_{T_{ref}} S_{solar} G_T [1 - 0.0045(T_{panel} - 298.15)] + n_{pipe} \frac{T_{panel} - T_w}{R_{pw}} \tag{23}$$

Here, S_{solar} is the area of solar array to receive solar irradiation. $\eta_{T_{ref}} S_{solar} G_T [1 - 0.0045(T_{panel} - 298.15)]$ is the energy which the solar

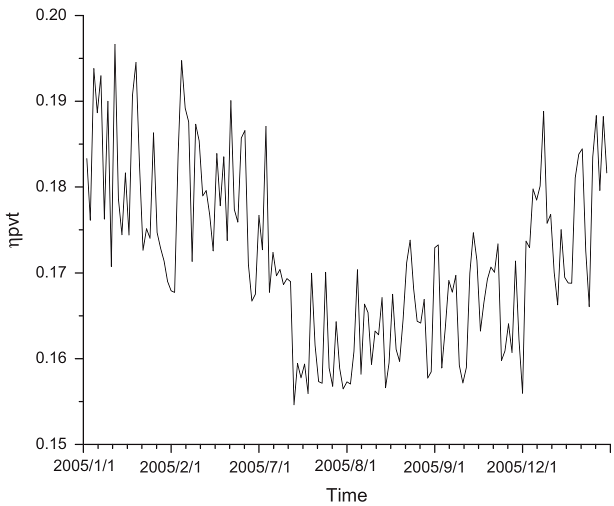

Fig. 14. Simulation electrical efficiency of heat pipe PV/T in summer and winter.

Table 5
the total cooling capacity in summer and heating capacity in winter.

	Total radition (KW h)	Average η_{pvt} (%)	COP	Total cooling capacity in summer/heating capacity in winter
Summer (July–September)	380.31	16.4	0.45	35.770(KW h)
Winter (December–February)	420.53	17.9	1.7	127.97

energy transferred to electric energy. $n_{pipe}\frac{T_{panel}-T_{w1}}{R_{pw}}$ is the heat which was transferred from PV/T panel to the water in storage tank.

The lost energy:

$$Q_{lost} = \kappa_{panel}S_{panel}\beta(T_{panel}^4 - T_{panel}^4) + (2.8 + 3.0u)S_{panel}(T_{panel} - T_{amb}) \tag{24}$$

β is the Boltzmann's constant. κ_{panel} is the emissivity of absorber panel. $\kappa_{panel}S_{panel}\beta(T_{panel}^4 - T_{amb}^4)$ is the radiation heat transferred between the panel and ambition. $(2.8 + 3.0u)S_{panel}(T_{panel} - T_{amb})$ is the convective heat transfer between the panel and ambition.

Buildings composited with thermoelectric cooling and heating systems driven by a heat pipe PV/T system can reduce cooling load in summer operation mode and heating load in winter operation mode. The electrical efficiency, total cooling capacity in summer and heating capacity in winter are calculated with the climate design data 2005 Hefei of china (Climate Design Data 2005 ASHRAE Handbook), and they are showed in Fig. 14 and Table 5.

6. Conclusion

Theoretical and experimental investigation on the winter operation mode of a thermoelectric cooling and heating system driven by heat pipe photovoltaic/thermal panel are presented in this paper. And the energy and exergy analysis of this system in summer and winter operation mode are also done. The result indicates that:

(1) In this case, the system has a good heating capacity, the electrical efficiency of the heat pipe PV/T panel is about 16.7%, the thermal efficiency of the system is about 23.5%.
(2) Based on calculation with the climate design data 2005 Hefei of China, one building composited with this system can provide cooling capacity about 35.77 KW h in summer season and heating capacity about 127.97 KW h in winter season in this case.
(3) As the ambition temperature and operation temperature are important factors, the energetic efficiency of this system in summer operation mode is higher than that in winter operation mode, but the exergetic efficiency of the heat pipe PV/T system in summer operation mode is lower than that in winter operation mode.

Acknowledgements

The work described in this paper has been supported by the Program for New Century Excellent Talents in University (NCET-11-0876) and the National Nature Science Fund of China (Project No. 51078342).

References

[1] Beikircher T, SpirkL W. Analysis of gas heat conduction in evacuated tube solar collectors. ASME J Solar Energy Eng 1996;118:157–61.
[2] Issa M, Kodah Z, Ai-Nimr MA. Further development of a v-trough solarconcentrator. Internet J Solar Energy 1990;8:81–96.
[3] Kudish AI, Evseev EG, Walter G, Leukefelds T. Simulation study of a solar collector with a selectively coated polymeric double walled absorber plate. Energy Convers Manage 2002;43:651–71.
[4] Smirnov SV, Moyseenko VV. The effect of heat radiation of a solar collector's absorbing surface elements on its efficiency. Appl Solar Energy 1995;3:172–8.
[5] Ji Jie, Luo Chenglong, Chow Tin-Tai, Sun Wei, He Wei. Thermal characteristics of a building-integrated dual-function solar collector in water heating mode with natural circulation. Energy 2011;36:566–74.
[6] Jie Ji, ChengLong Luo, Wei Sun, Wei He, Gang Pei, ChongWei Han. A numerical and experimental study of a dual-function solar collector integrated with building in passive space heating mode. Eng Thermophys 2010;55:1568–73.
[7] Ji J, Luo C-L, Chow T-T, Sun W, He W. Modelling and validation of abuilding-integrateddual-function solar collector. Proc Inst Mech Eng Part A J Power Energy 2011:225–59.
[8] Helmers Henning, Kramer Korbinian. Multi-linear performance model for hybrid (C) PVT solar collectors. Sol Energy 2013;92:313–22.
[9] Faizal M, Saidurb R, Mekhilefc S, Alimb MA. Energy, economic and environmental analysis of metal oxides nanofluid for flat-plate solar collector. Energy Convers Manage 2013;76:162–8.
[10] da Silva RM, Fernandes JLM. Hybrid photovoltaic/thermal (PV/T) solar systems simulation with Simulink/Matlab. Sol Energy 2010;84:1985–96.
[11] Fernández-Seara José, Piñeiro Carolina, Alberto Dopazo J, Fernandes F, Sousa Paulo XB. Experimental analysis of a direct expansion solar assisted heat pump with integral storage tank for domestic water heating under zero solarradiation conditions. Energy Convers Manage 2012;59:1–8.
[12] Moreno-Rodríguez A, González-Gil A, Izquierdo M, Garcia-Hernando N. Theoretical model and experimental validation of a direct-expansion solar assisted heat pump for domestic hot water applications. Energy 2012;45:704–15.
[13] Chaturvedi SK, Gagrani VD, Abdel-Salam TM. Solar-assisted heat pump – a sustainable system for low-temperature water heating applications. Energy Convers Manage 2014;77:550–7.
[14] Pei Gang Fu, Huide Zhu Huijuan, Jie Ji. Performance study and parametric analysis of a novel heat pipe PV/T system. Energy 2012;37:384–95.
[15] Rahbar N, Esfahani JA. Experimental study of a novel portable solar still by utilizing the heat pipe and thermoelectric module. Desalination 2012;284:55–61.
[16] Chávez-Urbiola EA, Vorobiev Yu V, Bulat LP. Solar hybrid systems with thermoelectric generators. Solar Energy 2012;86:369–78.
[17] Dai YJ, Wang RZ, Ni L. Experimental investigation on a thermoelectric refrigerator driven by solar cells. Renew Energy 2003;28:949–59.
[18] He Wei, Zhou Jinzhi, Hou Jingxin, Chen Chi, Ji Jie. Theoretical and experimental investigation on a thermoelectric cooling and heating system driven by solar. Appl Energy 2013;107:89–97.
[19] Jie J, Hua Y, Gang P, Bin J, Wei H. Study of PV-Trombe wall assisted with DC fan. Build Environ 2007;42:1522–44.
[20] Chow TT, Pei G, Fong KF, Lin Z, Chan ALS, Ji J. Energy and exergy analysis of photovoltaic–thermal collector with and without glass cove. Appl Energy 2009;86:310–6.
[21] Gang Pei, Guiqiang Li, Xi Zhou, Jie Ji, Yuehong Su. Experimental study and exergetic analysis of a CPC-type solar water heater system using higher-temperature circulation in winter. Sol Energy 2012;86:1280–6.
[22] Xu Desheng. Thermoelectric refrigeration and applications. Shanghai: Jiao Tong University Press; 1999.
[23] Weilan Gu, Yansheng Yang. The influence of temperature on contact resistance of metallic surfaces temperature. J Nanjing Univ Aeronaut Astronaut 1994;26:342–50.